Pharm Res (2017) 34:1428–1443
DOI 10.1007/s11095-017-2159-6

RESEARCH PAPER

An Efficient and Rapid Method to Monitor the Oxidative Degradation of Protein Pharmaceuticals: Probing Tyrosine Oxidation with Fluorogenic Derivatization

Rupesh Bommana [1] • Olivier Mozziconacci [1,2] • Y. John Wang [3] • Christian Schöneich [1]

Received: 17 January 2017 / Accepted: 3 April 2017 / Published online: 18 April 2017

ABSTRACT

Purpose The loss of potency of protein therapeutics can be linked to the oxidation of specific amino acid residues leading to a great variety of oxidative modifications. The comprehensive identification of these oxidative modifications requires high-resolution mass spectrometry analysis, which requires time and expensive resources. Here, we propose a fluorogenic derivatization method of oxidized Tyr and Phe yielding benzoxazole derivatives, as an orthogonal technique for the rapid screening of protein oxidation.

Methods Four model proteins, IgG1, human growth hormone (hGH), insulin and bovine serum albumin (BSA) were exposed to oxidation via peroxyl radicals and metal-catalyzed reactions and efficiently screened by fluorogenic derivatization of Tyr and Phe oxidation products. Complementary LC-MS analysis was done to identify the extent of methionine oxidation in oxidized proteins.

Results The Fluorogenic derivatization technique can easily be adapted to a 96-well plate, in which several protein formulations can be screened in short time. Representatively for hGH, we show that the formation of benzoxazole parallels the oxidation of Met to methionine sulfoxide which enables estimation of Met oxidation by just recording the fluorescence.

Conclusions Our rapid fluorescence based screening allows for the fast comparison of the stability of multiple formulations.

KEY WORDS fluorogenic derivatization · human growth hormone · mass spectrometry · monoclonal antibody · protein oxidation

Electronic supplementary material The online version of this article (doi:10.1007/s11095-017-2159-6) contains supplementary material, which is available to authorized users.

✉ Christian Schöneich
schoneic@ku.edu

[1] Department of Pharmaceutical Chemistry, University of Kansas, 2095 Constant Avenue, Lawrence, Kansas 66047, USA

[2] Present address: Analytical Sciences, Merck & Co., Inc., Kenilworth, New Jersey, USA

[3] Late Stage Pharmaceutical Development, Genentech, S. San Francisco, California 94080, USA

ABBREVIATIONS

AAPH	2, 2′-azobis (2-methylpropionamidine) dihydrochloride
ABS	4-(aminomethyl) benzenesulfonic acid
BMS	bis (2-mercaptoethyl) sulfone
BSA	Bovine serum albumin
DOCH	2-amino-3-(3, 4-dioxocyclohexa-1, 5-dien-1-yl) propanoic acid
DOPA	3, 4-dihydroxyphenylalanine
hGH	Human growth hormone
IAA	Iodoacetamide
IgG	Immunoglobulin G
LTQ-FT	Linear ion trap quadrupole-Fourier transform
MCO	Metal catalyzed oxidation
Q-TOF	Quadrupole time-of-flight
SEC	Size exclusion chromatography

INTRODUCTION

Protein pharmaceuticals represent a fast growing class of therapeutics. Since the development of the first recombinant protein pharmaceuticals in 1982, more than 170 biotherapeutic products have been introduced to treat various diseases such as cancer, autoimmune diseases, allergy, infectious diseases, inflammation and various genetic disorders (1–3). The global market for protein therapeutics is estimated to be worth $168

billion by 2017 (3). Much of the success of protein therapeutics is attributed to the influx of a large number of monoclonal antibodies into the pharmaceutical market (4).

One of the most demanding tasks in the development of biotherapeutics is to maintain physical and chemical stability (3). Protein unfolding, aggregation, surface adsorption and precipitation are major forms of physical instabilities encountered by protein therapeutics (3–6). Chemical modifications involve covalent changes of chemical bonds, which ultimately lead to the formation of new chemical structures. Deamidation and oxidation are among the major chemical modification pathways of protein pharmaceuticals (2,3).

Methionine (Met), cysteine (Cys), tryptophan (Trp), tyrosine (Tyr), phenylalanine (Phe) and histidine (His) are significantly more sensitive to a series of oxidation pathways, due to the high reactivity of sulfur and aromatic rings towards various reactive oxygen species (3–8). Frequently, the chemical modifications of these amino acid residues result in structural and biologic consequences. For example, the formation of methionine sulfoxide (MetSO) in human IgG1 can impact its serum half-life (9), conformational stability (5), and the binding affinity to protein A and protein G columns used for purification (10). Likewise, the oxidation of the other amino acids can also pose problems for the potency of protein pharmaceuticals. For example, the oxidation of a single Trp residue is responsible for the loss of binding and biological activity upon (UV) light irradiation in MEDI-493, a monoclonal antibody (mAb) against respiratory syntical virus (RSV) (11).

Peptide bond flexibility, protein conformation and surface accessibility of amino acids affect the oxidation rates of amino acid residues (8). Buffers, excipients, metal ions, light and temperature are also factors, which impact the oxidation pathways of proteins (3,5,8). Autoxidation of polysorbates results in the formation of hydroperoxides which can oxidize proteins (12). Polysorbates are the most common excipients used in protein formulations to prevent protein aggregation and protein surface adsorption (12,13). Trace amounts of metals can be accidentally introduced into protein therapeutics during manufacturing and formulation through leaching from metal containers and excipients respectively. (14). These trace amounts of metal ions can induce metal-catalyzed oxidation (15–17).

The oxidation of therapeutic proteins is monitored via a wide array of sensitive analytical techniques, including peptide mapping and mass spectrometry (4,18–21). While offering high resolution and information on product identity, these techniques are time-consuming.

The aim of this study is to implement a fluorogenic derivatization method of oxidized Tyr and Phe as an orthogonal technique for the rapid screening of protein oxidation, and to evaluate whether a quantitative correlation exists between the oxidation of Tyr/Phe and Met for a given protein and specific oxidation conditions. The oxidation of Tyr and Phe generates aromatic vicinal diols such as 3, 4 dihydroxyphenylalanine (DOPA) (16) which can be derivatized with benzylamine derivatives (22). Tryptophan oxidation yields several oxidation products, among them 5-hydroxy tryptophan (5-HTP), which can also be derivatized benzylamine derivatives (23). DOPA and 5-HTP react with 4-amino methyl benzenesulfonic acid (ABS) to form a highly fluorescent benzoxazole (Scheme 1; λ_{em} = 490 nm, λ_{ex} = 360 nm) (22,23). This method was initially developed to monitor oxidized proteins derived from tissue (22,23), but is here applied to the screening of protein pharmaceuticals. To demonstrate that this fluorogenic method can be used as a high-throughput assay to screen for the stability of proteins, we evaluated this method with four proteins (bovine serum albumin (BSA), human growth hormone (hGH), a monoclonal antibody (IgG1) and insulin) exposed to oxidation via peroxyl radicals and metal-catalyzed reactions, respectively. Peroxyl radicals ($ROO^{\bullet}$) were generated through the thermal decomposition of 2,2′-azobis (2-methylpropionamidine) dihydrochloride (AAPH) (25) (Scheme 2**)**, a process that mimics the oxidation of proteins by peroxyl radicals generated from polysorbates (24–26). Metal-catalyzed oxidation was initiated through the exposure of proteins to Cu (II)/L-ascorbic acid, or Fe (II)/H_2O_2 These conditions were selected to simulate the effect of trace amounts of metals inadvertently introduced into protein formulations during production and storage (17,27). The oxidized proteins were reacted with ABS and subsequently placed on a UV-transilluminator (Fotodyne Inc., Hartland, WI, USA) to visualize the fluorescent products. For quantitative screening, the samples were prepared in a 96 well plate in order to allow simultaneous comparison of all proteins and their different responses to different oxidative stresses. Representatively for hGH we also quantified MetSO by mass spectrometry, and we related the mass spectrometry quantification of MetSO to the ABS derived fluorescence. For this, representative ABS fluorescence charts were built by integrating MetSO (quantified by mass spectrometry) and ABS fluorescence (measured by fluorescence spectroscopy) to serve as a tool for the rapid prediction of MetSO formation for a given protein.

MATERIALS AND METHODS

IgG1 (14 mg/ml) and hGH were provided by Genentech, Inc. (San Francisco, CA. Recombinant insulin containing 0.4% (*w*/w) zinc was purchased from Roche Applied Science (Indianapolis, IN). BSA, AAPH, monobasic and dibasic sodium hydrogen phosphate (Na_2HPO_4 and NaH_2PO_4), ethylenediaminetetraacetic acid (EDTA), L-ascorbic acid, copper dichloride ($CuCl_2$), sodium chloride (NaCl), iron (II) sulphate ($FeSO_4$), guanidine hydrochloride, potassium ferricyanide $K_3Fe(CN)_6$, iodoacetamide (IAA), ammonium acetate

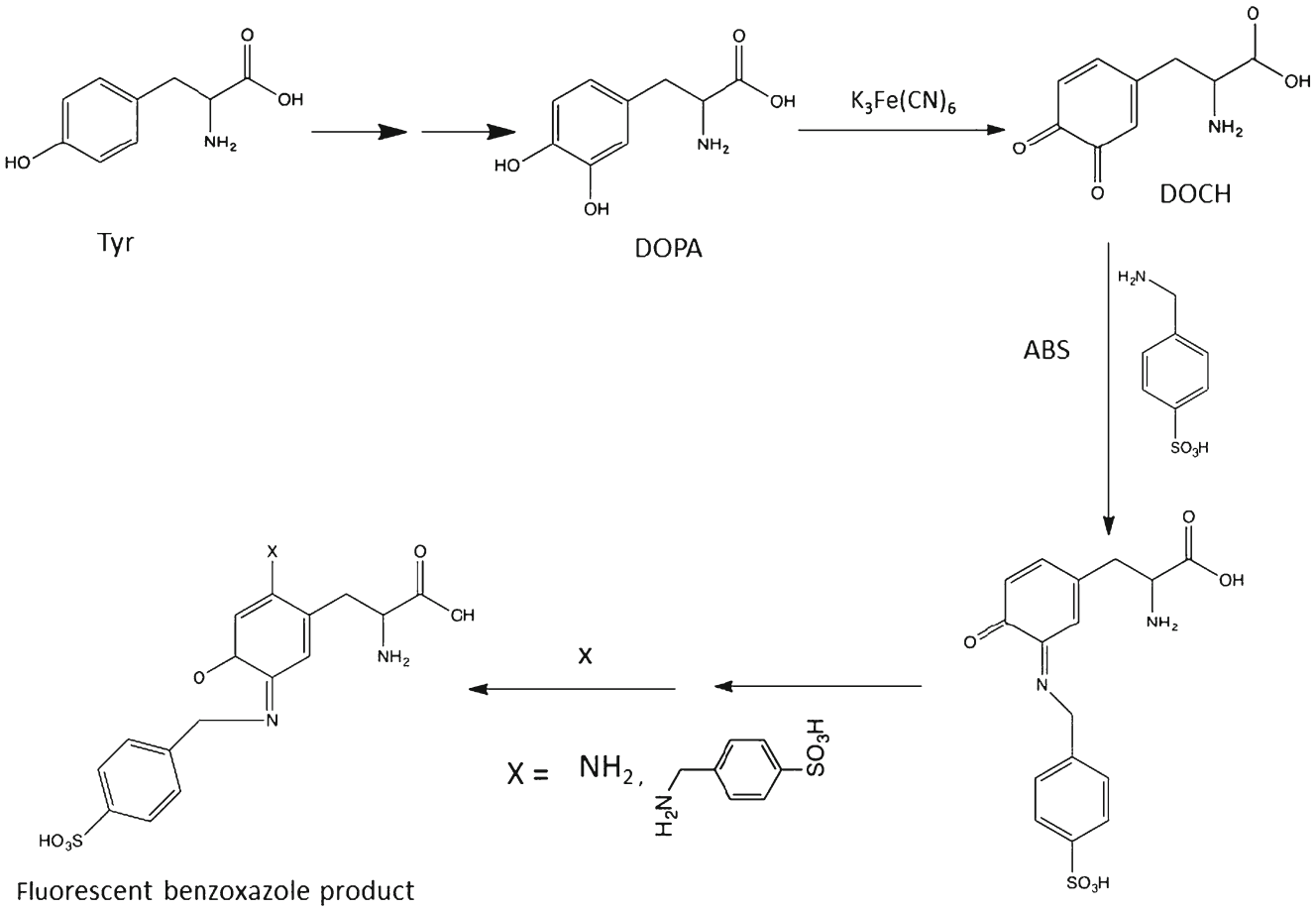

Scheme 1 Schematic representation of the fluorogenic derivatization of DOPA with ABS

($NH_4C_2H_3O_2$), ammonium bicarbonate (NH_4HCO_3), dithiothreitol (DTT), bis (2-mercaptoethyl) sulphone (BMS) and hydrogen peroxide (H_2O_2) were purchased form Sigma Aldrich (St. Louis, MO, USA). Trypsin/Lys-C, mass spectrometry grade, was purchased from Promega Corporation (Madison, WI, USA). SDS-PAGE running buffer (100 mM Tris, 1.92 M glycine and 0.1% (*w*/*v*) SDS at pH 8.25) and Precision plus Protein dual color standards were purchased from Bio-Rad (Hercules, CA, USA). Millipore Q water (milliQ water) was used for the preparation of all the solutions. Optimal water and acetonitrile (ACN), containing 0.1% (*v*/v) formic acid were purchased from Fisher Scientific (Waltham, MA). Amicon ultra-0.5 centrifugal filter devices equipped with a 10 kDa cut off membrane were purchased from Millipore Inc., (Bedford, MA, USA). 4-Aminomethyl-benzylsulfonic acid (ABS) was synthesized according to published protocol (22).

AAPH Oxidation

The model proteins (BSA, hGH, IgG1 and insulin) were dissolved at 1 mg/ml in 20 mM sodium phosphate buffer at pH 7.2. The reaction mixtures were prepared by mixing

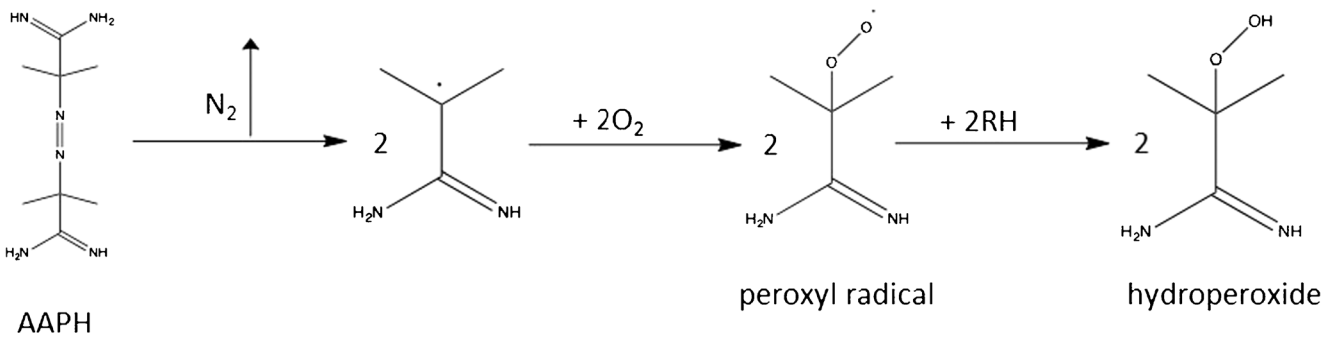

Scheme 2 Mechanism of thermolysis of AAPH, production and reaction of peroxyl radicals under aerobic conditions

200 µL of the model protein stock solution (1 mg/ml) with a series of concentrations of AAPH, and then incubated at 37°C for 3 h. The final concentrations of AAPH were 0 (control), 1, 2, 4, 8 and 16 mM. Based on the rate of radical generation at 37°C, 1.36 x 10^{-6} [AAPH] $Ms.^{-1}$, (25) a 3 h incubation with 16 mM AAPH generates a total of 2.35 x 10^{-4} M initial peroxyl radicals. With a concentration of hGH (1 mg/ml) at 4.5 x 10^{-5} M, the maximal ratio of [$ROO^{\bullet}$] / [hGH] = 5.2. To stop the reaction, the oxidized hGH samples were buffer exchanged with 100 mM phosphate buffer (pH 9.2) for 12 mins at 14,000 g (4°C, 3 times) using Amicon ultra- 0.5 centrifugal filters equipped with a 10kD cut-off membrane. In order to test whether we completely stopped the reaction we compared two samples (i) AAPH-exposed hGH, which was buffer exchanged, and (ii) AAPH-exposed hGH, which was buffer exchanged but incubated for 3 additional hours at 37°C. After derivatization with ABS, both samples showed the same fluorescence intensity, indicating that all AAPH had been removed by buffer exchange.

Metal Catalyzed Oxidation

Cu (II) /L-Ascorbate

Metal catalyzed oxidation of model proteins (1 mg/ml, in 20 mM sodium phosphate buffer, pH 7.2) by Cu (II)/L-ascorbic acid was performed by mixing model proteins with various concentrations of Cu (II) to reach final concentrations ranging from 5 µM to 20 µM. To allow binding of Cu (II) to the proteins, the samples were incubated with Cu (II) for ten minutes prior to the addition of L-ascorbic acid (29). After ten minutes, 500 µM of L-ascorbic acid was added to each sample. The final solution was incubated at 37°C for 3 h. The reactions were stopped by the addition of 50 µL of 50 mM EDTA.

Fe (II)/H_2O_2/EDTA

Separate stock solutions of EDTA (20 mM), Fe^{II} (10 mM), and H_2O_2 (10 mM) were prepared in Ar-saturated ammonium acetate buffers (20 mM, pH 7.2). 500 µL of the EDTA solution was mixed with 400 µL of the Fe^{II} solution in order to prepare a stock solution of EDTA/Fe^{II} at 1 mM. After mixing, the solution was again saturated with Ar. Subsequently 200 µL of the model protein stock solution (1 mg/ml, in 20 mM ammonium acetate buffer pH 7.2) was mixed with 10 µL of the Fe^{II}/EDTA solution, and the oxidation reaction was started by the addition of 10 µL of the H_2O_2 stock solution. The samples were incubated at 37°C for 3 h. The reactions were stopped by the addition 250 µL DTPA (1 mM), and 10 µL of catalase (25 µM).

Fluorogenic Derivatization

After exposure of the model proteins to AAPH and metal catalyzed oxidation, the oxidized proteins were buffer exchanged with 100 mM sodium phosphate buffer (pH 9.2) using Amicon ultra-0.5 centrifugal filter devices equipped with a 10 kDa cut-off membrane. The optimal conditions for the derivatization of DOPA in oxidized proteins with ABS were as follows: oxidized protein samples were mixed with $K_3Fe(CN)_6$ at a molar ratio of $K_3Fe(CN)_6$: protein =30:1 in the presence of 10 mM ABS and followed by incubation of samples in the dark for 90 min. The procedures for analysis of the derivatized samples are described in the next two sections.

Size Exclusion Chromatography (SEC)

SEC was performed on a Shimazdu HPLC system equipped with two Shimazdu LC-20AT pumps (Shimazdu, Columbia, MD) and coupled both to a photo-diode array detector (Prominence RF-20A, Shimazdu, Columbia, MD) and a fluorescence detector (RF-20A, Shimazdu, Columbia, MD). The samples (90 µL) were injected onto a TSK-GEL G3000swxl column (7.8 mm TD x 30 cm, 5 µm, Tosoh Biosciences, King of Prussia, PA, USA). The mobile phase consisted of 200 mM sodium phosphate buffer and 50 mM sodium chloride at pH 7.0, and was eluted through the column at a constant flow rate of 0.7 ml/min.

Steady-State Fluorescence Spectroscopy Analysis

The steady-state fluorescence of protein samples derivatized with ABS was measured with a Shimazdu RF-5301PC-spectrofluorophotometer equipped with a 1-cm quartz cuvette. Fluorescence measurements at λ_{em} = 490 nm (λ_{exc} = 360 nm) were acquired both in a 500 µL 1-cm quartz cuvette (Starna cell, Atascadero, CA 93422) and on a 96 well plate model, respectively. The excitation and emission bandwidths were set at 5 nm.

Reduction and Alkylation of hGH

Oxidized and control hGH samples were purified through Amicon ultra-0.5 centrifugal filter devices equipped with 10 kDa membranes. The purified hGH samples were reconstituted in 100 µL of ammonium bicarbonate buffer (50 mM, pH 7.5). The disulfide bonds were reduced by the addition of 50 µL BMS (5 mM stock solution in ACN), followed by incubation at 45°C for 30 min. The reduced cysteine residues were alkylated by the addition of 50 µL of IAA (25 mM in NH_4HCO_3 buffer 50 mM, pH 7.4), followed by incubation for 2 h at 37°C.

Trypsin/Lys-C Digestion of hGH

150 µl of reduced and alkylated hGH (1 mg/ml) were mixed with 700 µL $HClO_4$ (0.5 M). The samples were centrifuged at 16,000 g at 4°C for 20 min and the resulting pellet was washed twice with milliQ water. The pellet was reconstituted in 200 µL of NH_4HCO_3 buffer (50 mM, pH 8). The protein samples were digested with trypsin/Lys-C (3 µg) in NH_4HCO_3 buffer (50 mM, pH 8) at 37°C overnight. The proteolytic digests were purified using Amicon ultra-0.5 centrifugal devices equipped with 10 kDa membranes to separate undigested protein and trypsin/Lys-C from the tryptic peptides.

Sodium Dodecyl Sulfate Polyacrylamide gel Electrophoresis (SDS-PAGE) of hGH

After reduction and alkylation of Cys residues, 20 µL solution containing either native or oxidized hGH (1 mg/ml), and its control were mixed with 1.1 X reducing sample buffer, which consisted of 68.89 mM Tris HCl at pH 7.0, 2.2% *w*/w SDS, 0.044% *w*/w bromophenol blue, 22.22% *w*/w glycerol, and 111.11 mM DTT. The samples were boiled at 100°C for 2 min after mixing. An aliquot of 20 µL of each sample was loaded onto a 4–20% polyacrylamide gel from Bio-Rad (Hercules, CA, USA). Molecular weight standards and Precision Plus Protein Dual Color Standards (Bio-Rad) were also loaded onto the same gel. The gel electrophoresis was run at a difference of potential of 200 V for 40 min using 10-fold diluted running buffer. The fluorescence bands that contained protein derivatized with ABS, were visualized through a UV-transilluminator (λ = 302 nm).

In-Gel Digestion

The fluorescent bands were excised for in-gel digestion, according to the protocol described by Shevchenko *et al.* (30). Briefly, the gel slices were first rinsed twice with 100 mM NH_4HCO_3 (pH 7.8) in H_2O/ACN (1:1 *v*/v) and then rinsed with 100% ACN at room temperature. The gel slices were dried using a Speedvac from Labconco Corp. (Kansas City, MO, USA). The dried gel slices were incubated for one hour at 4°C in 200 µL of 50 mM acetic acid, containing 5 µg of sequencing-grade trypsin/Lys-C. An aliquot of 200 µL of 100 mM NH_4HCO_3 (pH 7.8) was then added to the samples prior to protein digestion. The samples were incubated at 37°C for 8 h. Upon completion of the digestion, the protein solutions were transferred into new 1.5-mL Eppendorf vials. The gel slices were rinsed three times with 100% ACN, and the rinsing solutions were combined with the solutions containing digested protein in the new Eppendorf vials. The samples were concentrated using the Speedvac to reach a final volume of 20 µL for LC-MS/MS analysis (30).

Mass Spectrometry Analysis

LC-ESI-MS experiments were performed on an nanoAcquity UPLC system (Waters Corporation, Milford, MA) coupled to either a Xevo Q-TOF (Waters Corporation, U.K) or a linear ion trap quadrupole-Fourier transform (LTQ-FT) mass spectrometer (Thermo-Finnigan, Bremen, Germany).

Xevo Q-TOF Mass Spectrometry Analysis

LC-MS analysis were performed on a Xevo Q-TOF mass spectrometer (Waters Corp.,U.K), equipped with a nanoAcquity (Waters Corp.,U.K) chromatograph and a BEH nanocolumn (75 µm x 150 mm C18, Waters Corp.). Aqueous (A) and organic (B) mobile phases consisted of optimal water and formic acid (FA) 99.9%: 0.1%, (v:v), and ACN and FA 99.9%: 0.1%, (v:v). Tryptic peptides were eluted within 70 min by increasing mobile phase B linearly from 3 to 35% (v:v) within the first 50 min, and by increasing the amount of B to 95% (v:v) within the following 20 min. The flow rate was 0.3 µl/min. The Xevo Q-TOF was operated in the MS^E mode with all lenses optimized on the $[M + 2H]^{2+}$ ion for the $[Glu]^1$ -fibrinopeptide B. The cone voltage was 25 V, and Argon was admitted to the collision cell. The spectra were acquired using a mass range of 150–2000 Da. The data were accumulated for 0.5 s per cycle. MS/MS measurements were performed by ramping the collision energy from 10 V to 40 V.

LTQ-FT Mass Spectrometry Analysis

Experiments were carried out on a linear ion trap quadrupole-Fourier transform (LTQ-FT) ion cyclotron resonance mass spectrometer. The instrument was operated in the data dependent acquisition (DDA) mode. All the lenses were optimized on the $[M + H]^+$ ion from leucine enkephalin. Tryptic digests were eluted on a non-porous Presto FF-C18 column (15 cm x 0.5 mm, 2 µm, Imtakt USA, Portland, USA) at a flow rate of 5 µl/min. The ESI source was operated with a spray voltage of 2.8 kV, a tube lens offset of 96 V and a capillary temperature of 200°C. The mobile phases consisted of water, ACN and FA at a ratio of 99.9%:0%:0.1%, (v:v) for solvent A and 0%:99.9%:0.1%, (v:v) for solvent B. The raw files from the FT-ICR measurements were read by the Xcalibur 2.0 software package (Thermo Scientific, Waltham, MA) and analyzed with MassMatrix (31).

Calibration Curves

A calibration curve for mass spectrometry analysis was built by plotting the peak areas of the Glu-Fib peptide against a series of known concentrations of the Glu-Fib peptide. Glu-Fib was provided as lyophilized powder, to which 0.1% FA in optimal water was added to bring the concentration to 100 µM. A

dilution series was prepared by addition of 0.1% FA in optimal water. Calibration curves were built with concentrations ranging from 2–2000 nM (Fig. 1a and b). The calibration curves were built using peptide peak intensity measurements, which involved extraction of ion chromatograms from the LC-MS runs of the Glu-Fib peptide followed by calculation of peak areas. Calibration curves were built by plotting peak areas of the extracted ion chromatograms *versus* the theoretical concentrations. In the calibration curves, the slopes are representative of the sensitivities of the mass spectrometry method used for the analytes. The precision of the data was determined by measuring 3 replicates of one sample, which is represented by standard deviation. The two calibration curves were built to bracket the limit of quantification and the upper limit of linearity. Limit of quantification (LOQ, 5 nM) is the lowest concentration of the analyte that can be quantified. The upper limit of linearity (LOL, 2000 nM) describes the highest concentration of analyte above which linearity cannot be established between concentration and peak area (32).

The use of a 96-Microplate to Efficiently Monitor Oxidized Proteins by ABS Derivatization

To assess the presence of oxidized proteins in a large variety of protein samples we performed the fluorogenic derivatization with ABS in a 96 well microplate. BSA (1 mg/ml), IgG1 (1 mg/ml), insulin (1 mg/ml) and hGH (1 mg/ml) were oxidized with either AAPH (33), Fe(II)/H_2O_2/EDTA, or Cu(II)/L-ascorbate (33–35). After incubation, the samples were buffer exchanged with 100 mM sodium phosphate buffer (pH 9). Samples were centrifuged at 14,000 g for 12 min in Amicon 0.5-ultra filters equipped with 10kD cut-off membranes. After the centrifugation, samples were measured for protein concentration and adjusted accordingly before loading the samples into the well plate. 200 µL of each sample was transferred to a 96 well microplate. After loading the oxidized samples to the microplate, 50 µL of 60 mM ABS stock solution was added to the samples at final concentrations of 10 mM ABS, followed by the addition of 50 µL of 3 mM $K_3Fe(CN)_6$ stock solution to a final concentration of 500 µM. After 90 min, the microplate was placed on a UV-Transilluminator (operated at λ = 302 nm) for visualization of the fluorescence, and subsequently placed in a spectrofluorometer to read the absolute intensities.

RESULTS

The two objectives of this study were to establish a rapid screening method for Tyr and Phe oxidation and to evaluate whether there is a quantitative relationship between the oxidation of Tyr/Phe and Met for a given protein (representatively hGH) and a given oxidative stress system (representatively AAPH). Tyr/Phe oxidation to DOPA can easily be monitored by fluorescence detection after ABS derivatization of DOPA, while the oxidation of Met to MetSO must be monitored by HPLC coupled to either UV or mass spectrometry detection.

The results section is divided into four sub-sections. First, we will present the results on hGH alone, along with the details regarding the derivatization of DOPA by ABS. In the second sub-section, we will characterize the formation of MetSO in oxidized hGH. The third sub-section will focus on the development of ABS fluorescence charts to relate the quantification of MetSO by LC-MS to the fluorescence detection of DOPA in oxidized hGH. Finally, the development of a high-throughput assay to simultaneously screen for the oxidative degradation of a series of model proteins will be described.

ABS Derivatization to Monitor the Formation of DOPA in Oxidized hGH

After ABS derivatization of hGH oxidized with AAPH, we observed the formation of the fluorescent benzoxazole (λ_{em} = 490 nm on excitation at λ_{exc} = 360 nm) (Fig. 2, blue, a). The control (non-oxidized hGH), which underwent the same protocol for ABS derivatization showed little fluorescence (Fig. 2, black, b).

The ABS-dependent fluorescence intensity increases with the increase in concentration of AAPH (1 mM to 16 mM) used to oxidize hGH, indicating an AAPH-dependent increase of Tyr/Phe oxidation (Fig. 3). However, this increase is not linear over the range of AAPH concentration suggesting different sensitivity of different Phe/Tyr residues to AAPH derived oxidation. Similar observations were made by SEC analysis and fluorescence detection (Fig. 4, Fig. S3). HGH degradation induced by AAPH was monitored using SEC coupled to a diode array detector (Fig. S4), indicating an increase in aggregation with increasing AAPH concentration.

SDS-PAGE Analysis of ABS-Derivatized Oxidized hGH

After the incubation of hGH with different initial concentrations of AAPH (ranging from 1 mM to 16 mM), the protein was derivatized with ABS, followed by reduction and alkylation of derivatized hGH. The samples were then fractioned by SDS-PAGE.

The fluorescence intensity increased from lane 2 to lane 7 (Fig. 5) for both monomers and dimers (covalent aggregates) of hGH, which indicates the presence of oxidized Tyr and / or Phe that are derivatized with ABS, in both monomer and dimer. In addition, as we progress from lane 2–7, a smear of fluorescence starts to appear in the higher molecular weight region indicating the formation of higher

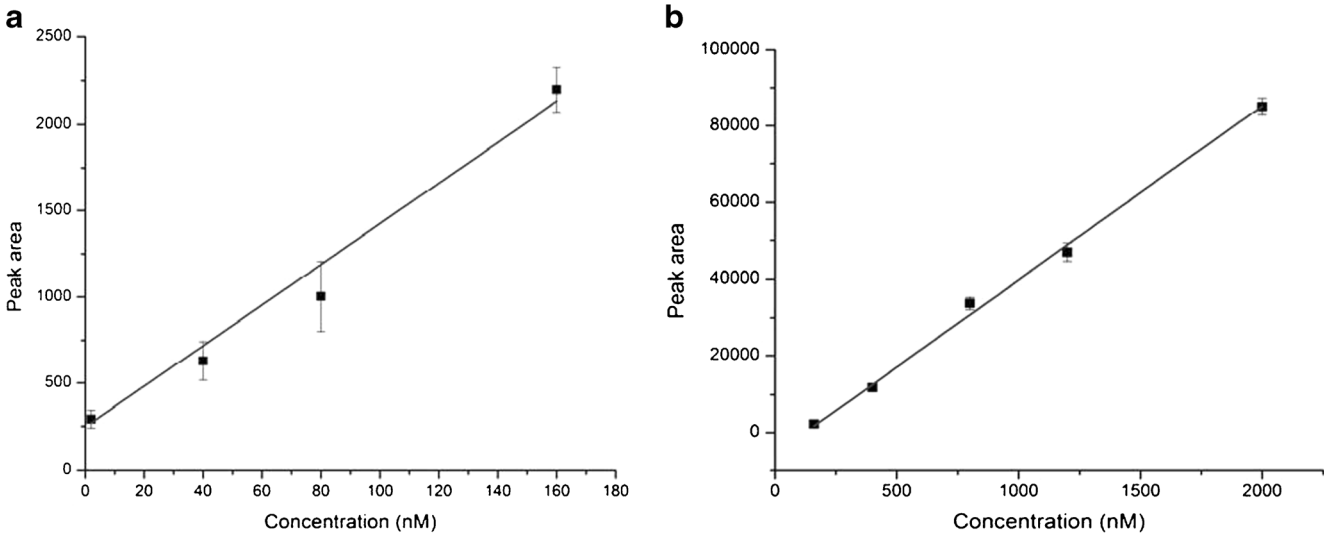

Fig. 1 Calibration curves obtained on Xevo-QTOF, using Glu-Fib standard peptide. (**a**) Glu-Fib concentration: 2–160 nM. (**b**) Glu-Fib concentration: 160–2000 nM.

molecular weight aggregates with oxidized Tyr and / or Phe. These observations confirm that the formation of DOPA increases with the increase in the initial concentration of AAPH.

Identification of DOPA and ABS Derivatized Peptides

The most intense fluorescent bands (corresponding to monomers) from the SDS–PAGE were excised and subjected to in-gel digestion, and the tryptic peptides were extracted and analyzed by LC-MS/MS. After oxidation of hGH, MS/MS analysis of the proteolytic peptides indicates hydroxylation of Tyr-35 in the tryptic peptide QEFEEAYIPK, where the fragment ions y3, y4, b5, and b6 demonstrate an increase of +16 Da of Tyr-35 (Fig. 6). After ABS-tagging of oxidized hGH, the LC-MS analysis of the tryptic digest revealed that the mass of the peptide QEFEEAYIPK increased by +197 Da, as expected for derivatization of DOPA with ammonia and ABS. The MS/MS spectrum confirms the conversion of Tyr 35 into benzoxazole (Fig. 7) and the structure is shown in the insert of Fig. 7. Indeed, the parent ion with m/z of 1450.39 corresponds to an increase of +197 Da in comparison to the original tryptic peptide QEFEEAYIPK. The series of y1-y4, and b1-b4 fragment ions indicate that the mass increase of 197 Da is located at Tyr-35. We also detected derivatization of DOPA with two ABS molecules (Fig. 8), consistent with the reaction mechanism of ABS derivatization (22,23). This twofold derivatized parent ion with m/z 1620.39

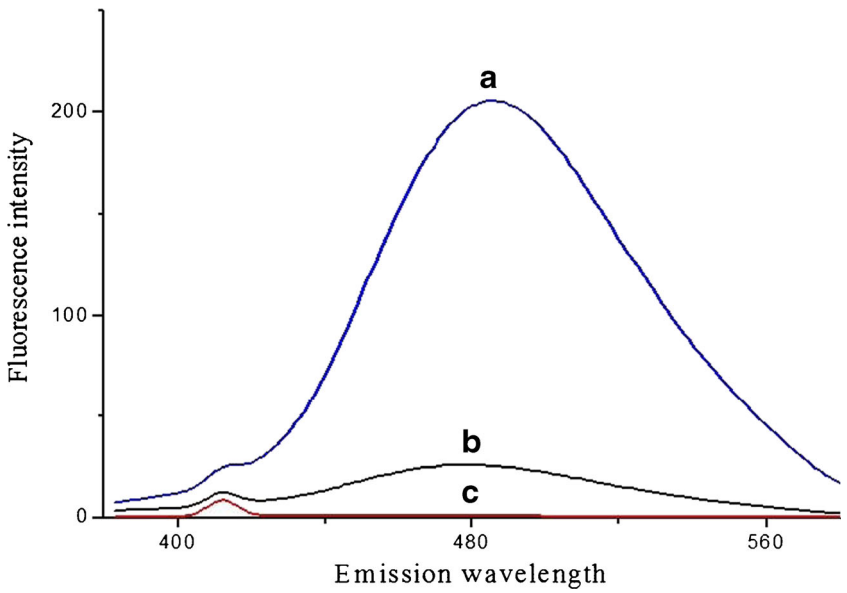

Fig. 2 Steady state fluorescence monitored after ABS derivatization of (**a**) hGH oxidized with 2 mM AAPH at 37°C for 3 h (*blue*), (**b**) non-oxidized hGH (*black*), (**c**) the background fluorescence of the hGH oxidized with 2 mM AAPH for 3 h at 37°C, prior to ABS derivatization (*red*).

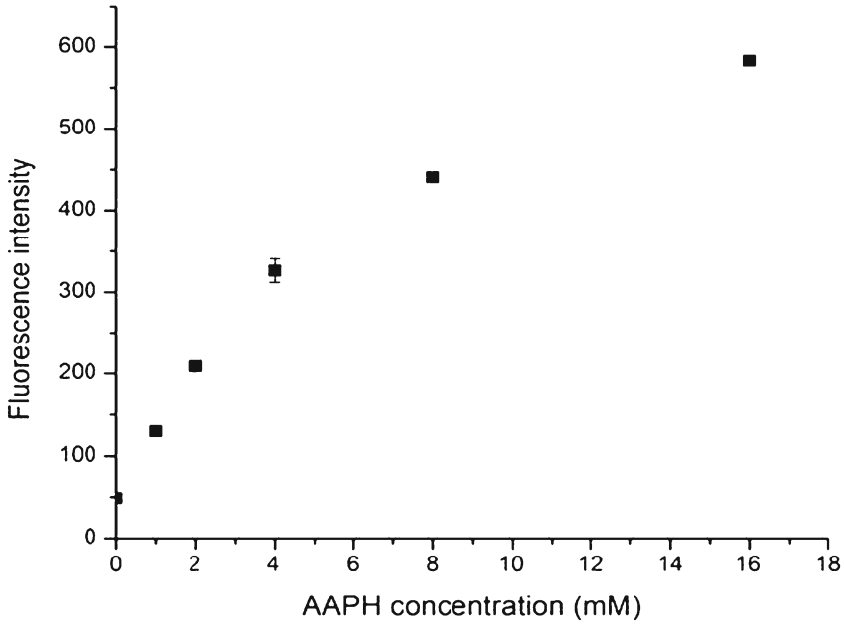

Fig. 3 Fluorescence (λ_{em} max) after ABS derivatization of hGH (1 mg/ml), oxidized in the presence of different initial concentrations of AAPH ranging from 0 (non-oxidized) to 16 mM, at 37°C for 3 h and monitored by steady-state fluorescence as shown in Fig. 2.

corresponds to an increase of +366 Da relative to the original tryptic peptide QEFEEAYIPK. This tryptic peptide originally contains also Phe, which is an additional potential target for oxidation (14). The series of y5-y8 and b1-b3 fragment ions shows no sign of derivatization at the original Phe-32 residue. The increase of +366 Da is located between the fragment ions y3 and y4, demonstrating that the addition of two molecules of ABS occurred at the original Tyr-35 residue. We observe no significant oxidation of Tyr-103 under our reaction conditions. However, this is not surprising as low yields of Tyr-103 oxidation were previously observed for much stronger oxidizing conditions, where [ROO•] / [hGH] = 30 (28). In contrast, under our experimental conditions, [ROO•] / [hGH] = 5.2.

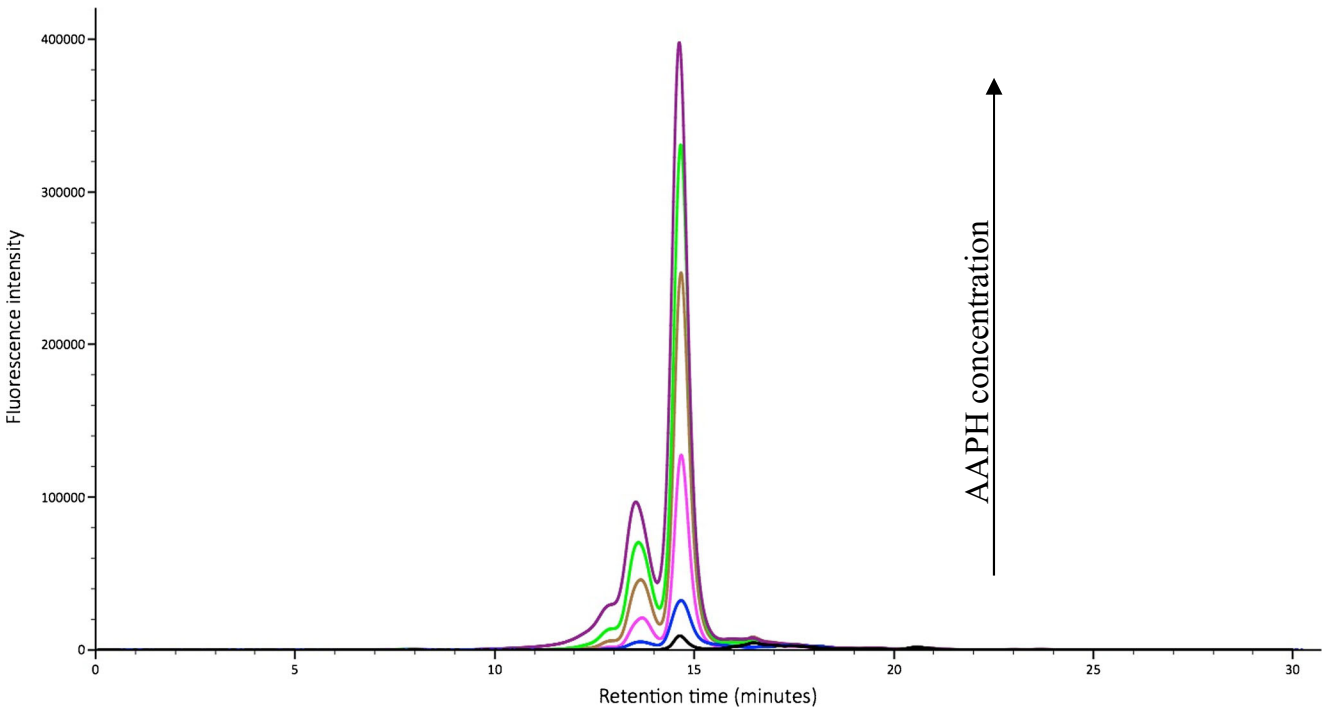

Fig. 4 Size exclusion chromatography (SEC) of ABS tagged oxidized hGH (1 mg/ml). Fluorescence detection (Ex **360 nm**-Em **490 nm**) of (**a**) non-oxidized but ABS-derivatized (*black*), oxidized hGH obtained after incubation of hGH with (**b**) 1 mM AAPH (*dark blue*), (**c**) 2 mM AAPH (*pink*), (**d**) 4 mM AAPH (*brown*), (**e**) 8 mM (*green*) and with (**f**) 16 mM AAPH (*purple*) for 3 h at 37°C.

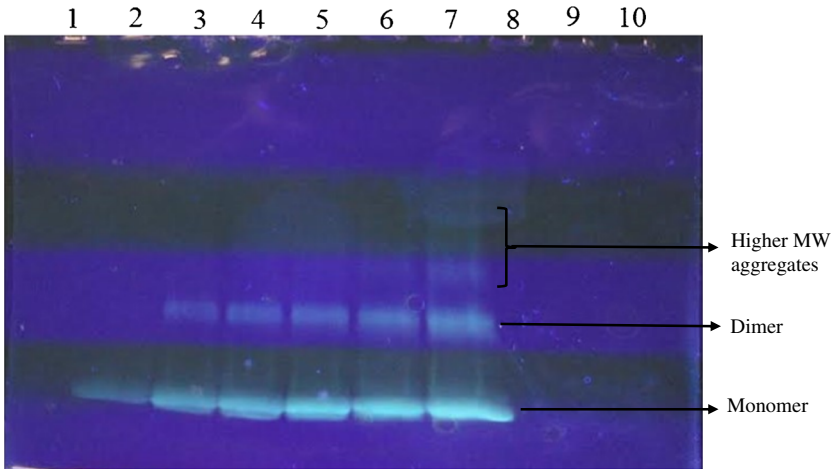

Fig. 5 SDS-PAGE analysis (reducing conditions) and fluorescence visualization of oxidized hGH (1 mg/ml) after ABS derivatization. Fluorescence was recorded by UV Transilluminator (Lane-1: molecular weight standards, Lane-2 hGH non-oxidized (control), Lane-3: hGH oxidized with 1 mM AAPH, Lane-4: hGH oxidized with 2 mM AAPH, Lane-5: hGH oxidized with 4 mM AAPH, Lane-6: hGH oxidized with 8 mM AAPH, Lane-7: hGH oxidized with 16 mM AAPH, Lane-8: derivatization reagents, Lane-9 and 10: empty

Identification of MetSO by LC-MS

hGH is a single chain protein consisting of 191 amino acids residues which contains three Met residues Met-14, Met-125, and Met-170 (Table I). Only Met-14 and Met-125 were oxidized to MetSO with significant yields after incubation of hGH with various concentrations of AAPH (28).

After oxidation of hGH, the MS/MS spectrum of the tryptic peptide LFDNAMLR showed that Met-14 was oxidized to MetSO. The fragment ions y3 and b6 confirm an increase of +16 Da at Met-14 (Fig. 9). Our analysis also revealed that Met-125 in the tryptic peptide DLEEGIQTLMGR was oxidized to MetSO**.** The latter was demonstrated by its MS/MS spectrum, which indicated through the formation of the y3 and b10 fragment ions that oxidation, occurred at Met-125 (Fig. 10).

MetSO in oxidized hGH was quantified as follows: The sum of the ion intensities of the oxidized tryptic peptides

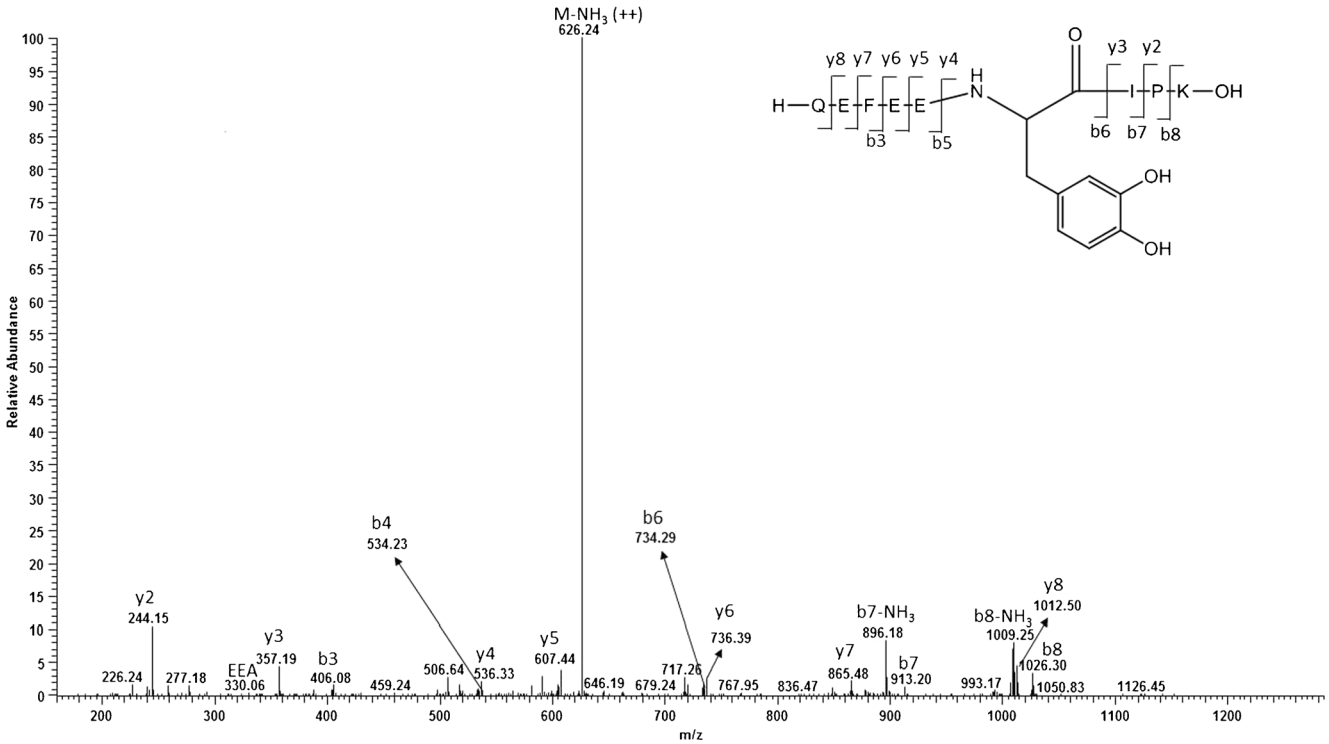

Fig. 6 Collision-induced dissociation (CID) obtained on an FT-LTQ mass spectrometer of the oxidized tryptic peptide QEFEEY (+16 Da) IPK.

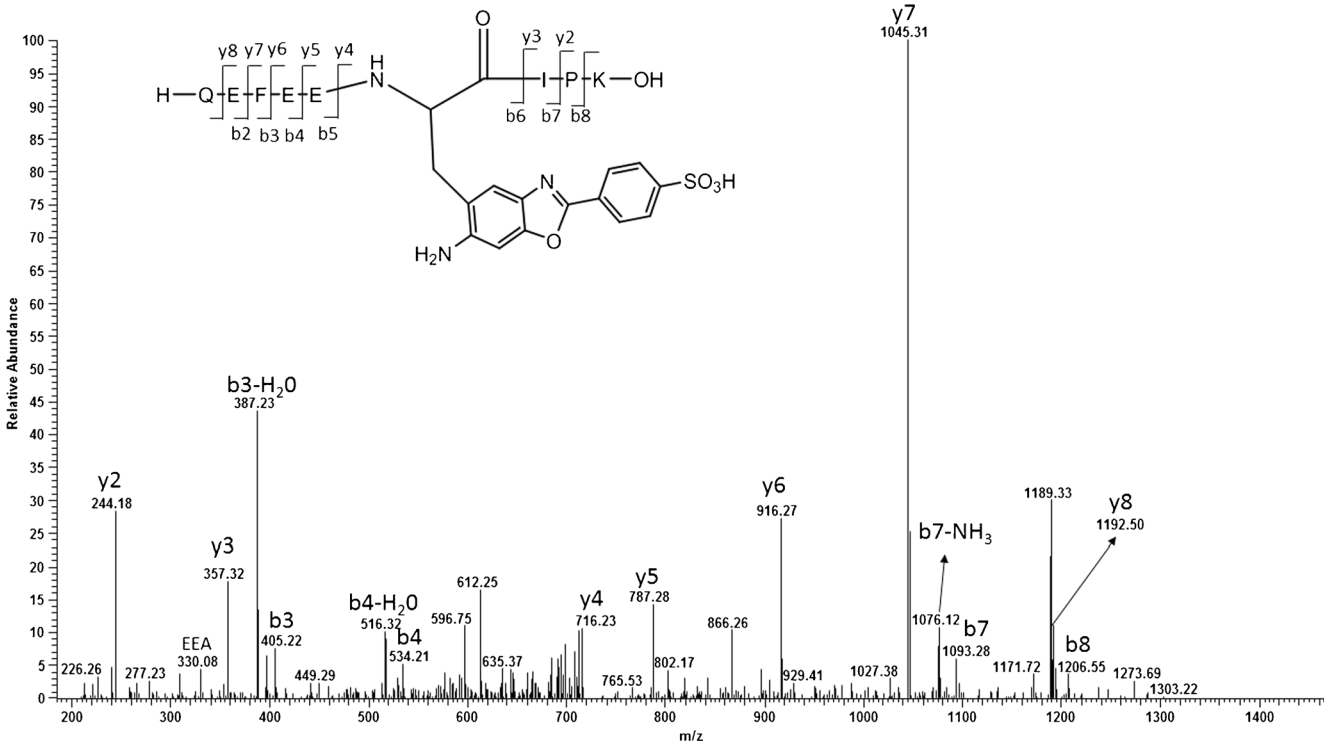

Fig. 7 Collision-induced dissociation (CID) obtained on an FT-LTQ mass spectrometer of the tryptic peptide QEFEEY(+197 Da)IPK, generated through oxidation and ABS derivatization of hGH.

LFDNA(MetSO)LR and DLEEGIQTL(MetSO)GR was compared to the Glu-Fib calibration curve (Fig. 11). To compensate any potential variation of the amount of MetSO to the variability of the recovery of the peptides after digestion,

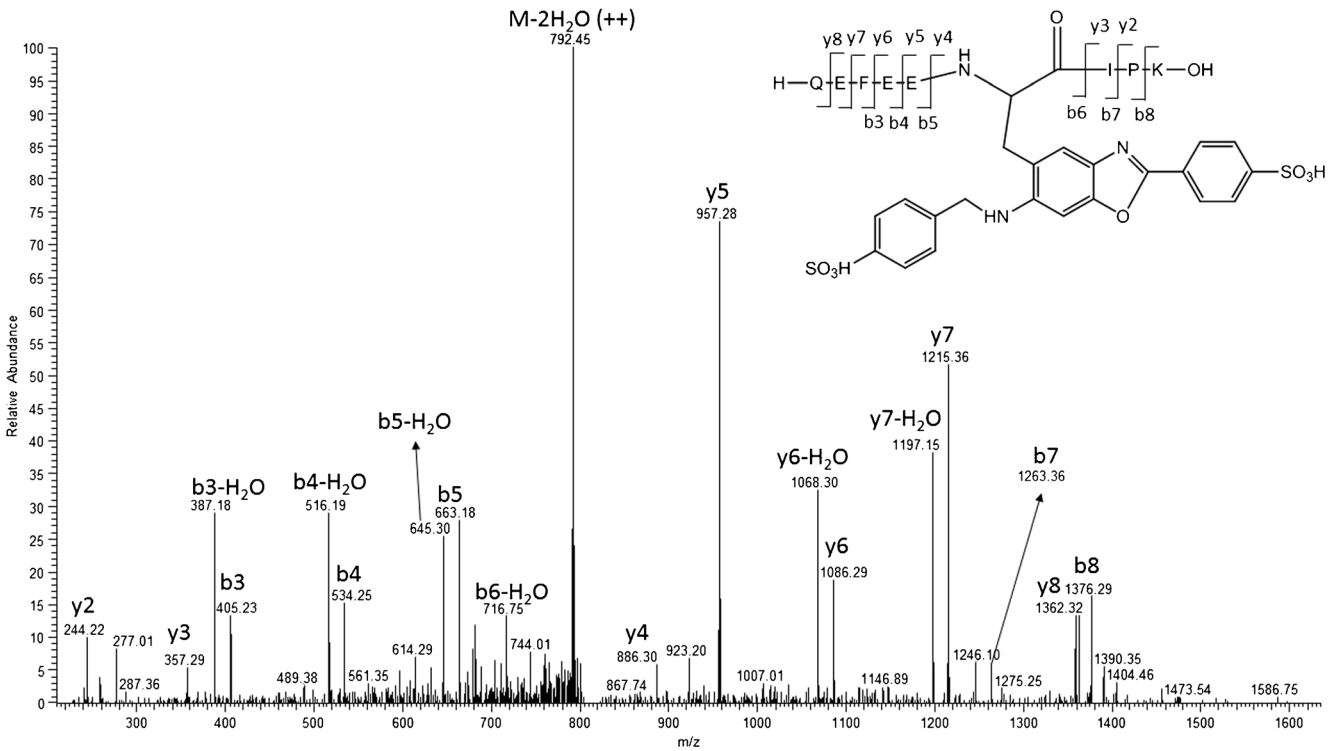

Fig. 8 Collision-induced dissociation (CID) obtained on an FT-LTQ mass spectrometer of the tryptic peptide QEFEEY(+366 Da)IPK, generated through oxidation and ABS derivatization of hGH.

Table I List of Methionine Containing Tryptic Peptides Obtained After Digestion of hGH with trypsin/Lys-C

Methionine	Tryptic peptide	m/z
Met-14	LFDNAMLR	979.50
Met-125	DLEEGIQTLMGR	1361.67
Met-170	DMDKVETFLR	1253.61

the MetSO containing peptides were normalized to the intensity of the oxidation resistant peptide SNLELLR. Quantification of MetSO was achieved assuming that MetSO containing peptides ionized similarly than the Glu-Fib peptide during ESI.

Correlation of DOPA Fluorogenic Derivatization with MetSO Formation in Oxidized hGH

The steady-state fluorescence intensities of ABS-derivatized hGH were plotted against the amount of MetSO detected by LC-MS (Fig. 12). The plot shows two distinct regions: for fluorescence intensities up to ca. 330 au, a ca. 6.6-fold increase in fluorescence (between ca. 50 and 330 a.u.) is accompanied by a ca. 5-fold increase in MetSO. However, for fluorescence intensities between 330 and 600 a.u., a < 2-fold increase in fluorescence intensity is accompanied by an almost 3-fold increase in MetSO. The existence of these specific regions can be rationalized by different sensitivities of various Tyr and Met residues towards oxidation. Nevertheless, these charts containing plots of fluorescence *vs.* MetSO permitted to predict the amount of MetSO without performing an LC-MS analysis. The robustness of this method was tested by the incubation of hGH with various AAPH concentrations which were not used to build the fluorescence *vs.* MetSO plots. For example, hGH was oxidized in presence of 7 mM AAPH for 3 h at 37°C. The oxidized hGH was reacted with ABS and the measured fluorescence intensity of 370 au was used to estimate the amount of MetSO to 1.6 nanomoles (± 0.054). This value for MetSO was reasonably close to the yield of MetSO 1.705 nanomoles (± 0.019) independently determined by mass spectrometry. We note, that a fluorescence chart built for one specific protein cannot be used to predict the oxidation of another protein, due to differences in sequence and, most likely, in the sensitivities of Met and Tyr to oxidation in different proteins. Hence, separate fluorescence charts have to be constructed for individual proteins.

High-Throughput Fluorescence Visualization of ABS Derivatized Protein Samples by UV-Transilluminator

The model proteins (hGH, IgG1, insulin and BSA) were exposed to various oxidation conditions, followed by derivatization with ABS and fluorescence visualization on the UV-

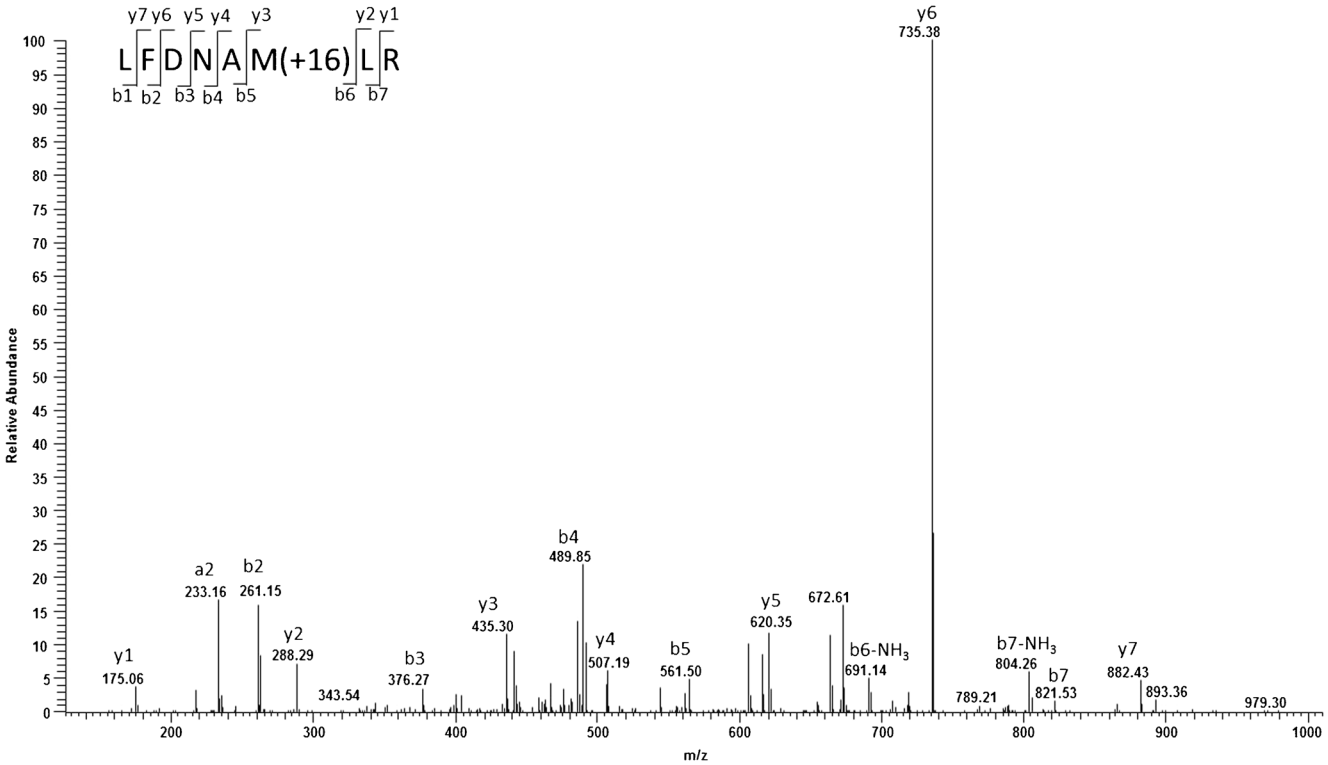

Fig. 9 Collision-induced dissociation (CID) obtained on an FT-LTQ mass spectrometer of the oxidized tryptic peptide LFDNAM (+16 Da) LR. The peptide is the result of tryptic digestion of oxidized hGH.

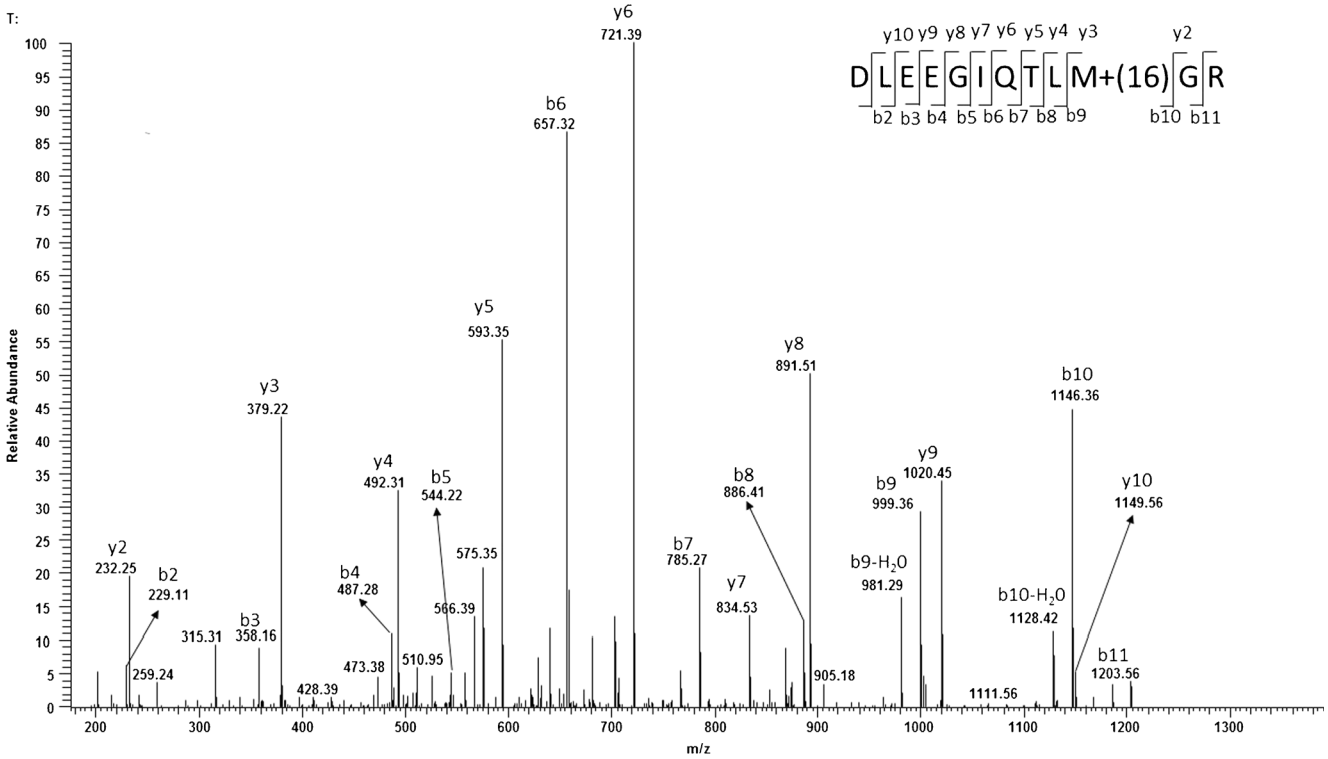

Fig. 10 Collision-induced dissociation (CID) obtained on an FT-LTQ mass spectrometer of the oxidized tryptic peptide DLEEGIQTLM (+16 Da) GR. The peptide is the result of tryptic digestion of oxidized hGH.

Transilluminator. Experiments were performed in a 96 well plate (one entire column on the microplate was loaded with the same protein). Model proteins exposed to AAPH, Cu (II)/L-ascorbate and Fe (II)/H_2O_2 were loaded to columns 1–4, 6–9 and 10–12, respectively in the microplate (Fig. 13). The first two wells in column 5 (5a and 5b) were loaded with derivatization reagents alone (ABS and $K_3Fe(CN)_6$) to monitor the background. Rows a and e were always loaded with non-oxidized (control) proteins exposed to derivatizing conditions with ABS. Table II presents the individual conditions for each well. Upon visualization (Fig. 13), protein samples that were exposed to stronger oxidation conditions always showed stronger fluorescence intensities as compared to

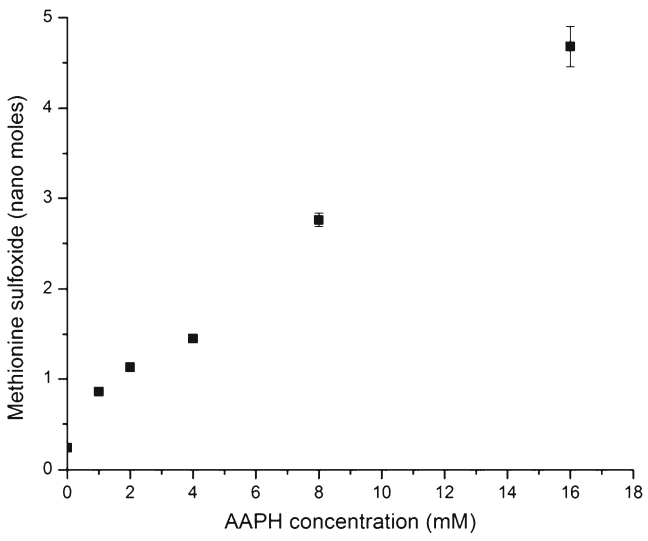

Fig. 11 LC-MS analysis: Formation and quantification of MetSO during oxidation of hGH by serial concentration of AAPH ranging from 0 (non-oxidized) to 16 mM on incubation for 3 h at 37°C. The data points represent the mean of four different experiments ± standard deviation.

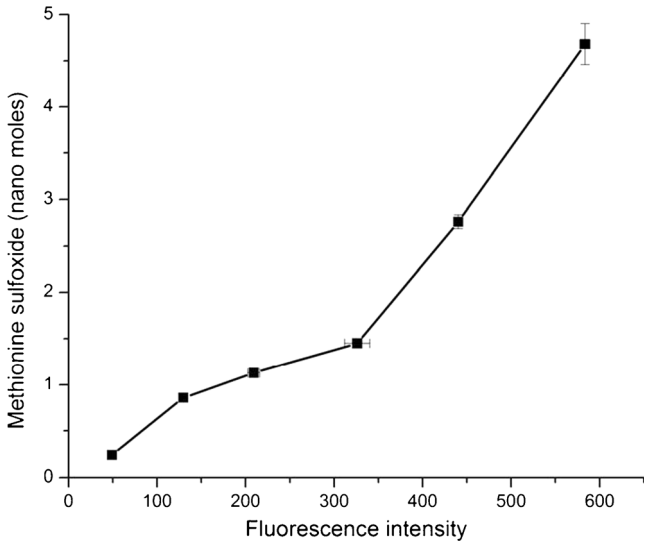

Fig. 12 ABS fluorescence chart acquired after plotting fluorescence of ABS tagged DOPA against the amount of MetSO detected by LC-MS in hGH oxidized with increasing concentration of AAPH incubated at 37°C for 3 h. Each data point represents the mean of four different experiments ± standard deviation.

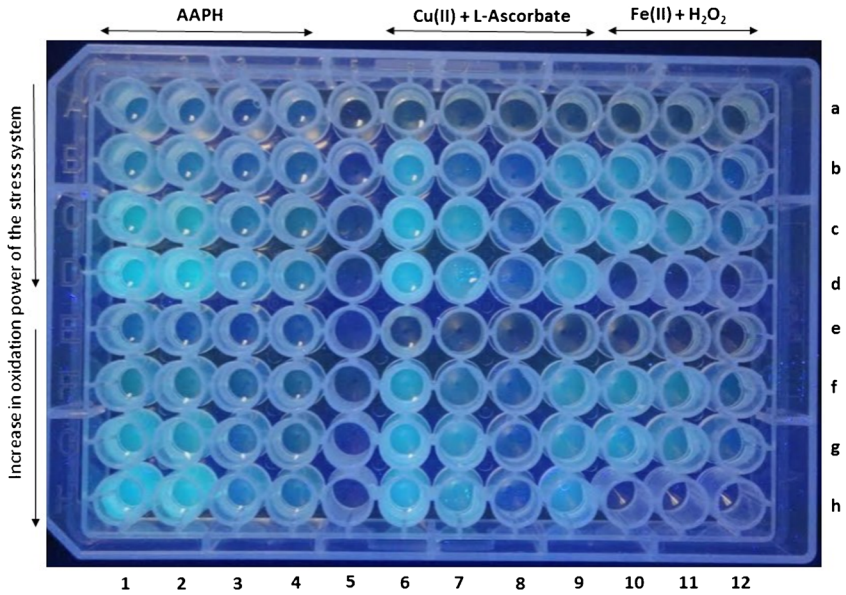

Fig. 13 Fluorescence visualization on a UV-Transilluminator ($\lambda = 302nm$). IgG1, hGH, Insulin and BSA protein samples were oxidized with respective oxidative stressing systems and derivatized with ABS. **1a** hGH control, **1b-1d** hGH oxidized with 1, 4, 8 mM AAPH respectively, **2a** IgG1 control, **2b-2d** IgG1 oxidized with 1, 4, 8 mM AAPH respectively, **3a** Insulin control, **3b-3d** Insulin oxidized with 1, 4, 8 mM AAPH respectively, **4a** BSA control, **4b-4d** BSA oxidized with 1, 4, 8 mM AAPH respectively. **5a** tagging reagents, **5b** 100 mM dibasic sodium phosphate buffer. **6a** hGH control, **6b-6d** hGH oxidized with 5, 10, 15 μM Cu (II) respectively and 500 μM L-Ascorbic acid, **7a** IgG1 control, **7b-7d** IgG1 oxidized with 5, 10, 15 μM Cu (II) respectively and 500 μM L-Ascorbic acid, **8a** Insulin control, **8b-8d** Insulin oxidized with 5, 10, 15 μM Cu (II) respectively and 500 μM L-Ascorbic acid, **9a** BSA control, **9b-9d** BSA oxidized with 5, 10, 15 μM Cu (II) respectively and 500 μM L-Ascorbic acid. **10a** hGH control, **10b-10c** hGH oxidized with 10, 20 μM Fe (II) + H_2O_2, **11a** IgG1 control, **11b-11c** IgG1 oxidized with 10, 20 μM Fe (II) + H_2O_2, **12a** Insulin control, **12b-12c** Insulin oxidized with 10, 20 μM Fe (II) + H_2O_2.

protein samples exposed to lower levels or no oxidation. There was minimal fluorescence in the non-oxidized controls. The fluorescence intensities of the ABS-derivatized samples are presented in the Supplementary Material (Fig. S5).

DISCUSSION

The length and intricacy of the development process for protein pharmaceuticals require the development of fast and affordable stability tests. The latter have already been developed for screening products, ranging from early stage (36) to late stage formulation development (37). The benefits of high-throughput screening rely on a rapid analysis, which permits to collect a substantial amount of data to preclude the release of unstable products. In the pharmaceutical industry any process, which can fulfill these requirements can help in introducing protein pharmaceuticals faster into the market. Another advantage of high-throughput screening is the possibility to analyze a broad variety of samples (e.g. different proteins) at the same time (36,37).

We have developed a quick and sensitive chemical assay to monitor the level of oxidation of proteins. Our assay is based on the derivatization of DOPA with ABS, which specifically allows for the detection of oxidation products of Phe and Tyr (14,22,23). We adapted our assay to a 96 well microplate framework, where four different non-oxidized (control) and oxidized model proteins (IgG1, insulin, hGH and BSA) were ABS-derivatized in a single microplate. The latter was placed on a UV-Transilluminator to reveal the specific fluorescence of the benzoxazole product, which resulted from the reaction between DOPA and ABS. This plate could also be read in a high throughput fashion on a fluorescence plate reader. The fluorescence values could be correlated to a previously generated interpolation curve like has been made for hGH.

Model proteins were exposed to increasing amounts of peroxyl radicals ($ROO^{\bullet}$), which were generated by thermolysis of AAPH in air saturated aqueous solution at a rate of 1.36×10^{-6} [AAPH] $Ms.^{-1}$ (38). Our assay correlates the increase of fluorescence intensities, resulting from the derivatization of DOPA by ABS, with the exposure of proteins to increasing amount of $ROO^{\bullet}$ (Fig. 3). Based on a calibration curve generated by Sharov *et al.*, (22) the amount of DOPA generated on hGH by exposure to increasing amounts of peroxyl radicals from AAPH was estimated to be between 1.02 p moles (1.1 µmoles per mole of protein) and 6.1 p moles (6.66 µmoles per mole of protein). Under our experimental conditions, the latter corresponds to a fluorescence intensity between 70 and 600 a.u. on our plate reader. Therefore, under our experimental conditions the ratio of Met oxidation over Tyr/Phe oxidation in hGH, was ca. 767:1. We also did observe DOPA by LC-MS analysis but its level was below the limit of quantification by MS.

Table II 96-Well Plate Loaded with IgG1, hGH, Insulin and BSA Oxidized Under the Indicated Conditions and Derivatized with ABS. The Symbol "-"Indicates Empty Wells

hGH control	IgG1 control	Insulin control	BSA control	tagging reagents	hGH control	IgG1 control	Insulin control	BSA control	hGH control	IgG1 control	Insulin control	a
hGH + 1mM AAPH	IgG1 + 1mM AAPH	Insulin + 1mM AAPH	BSA + 1mM AAPH	tagging reagents	hGH 5μM Cu(II) + 500μM L-Asc	IgG1 5μM Cu(II) + 500μM L-Asc	Insulin 5μM Cu(II) + 500μM L-Asc	BSA 5μM Cu(II) + 500μM L-Asc	hGH 10μM Fe(II) + 500μM H_2O_2	IgG1 10μM Fe(II) + 500μM H_2O_2	Insulin 10μM Fe(II) + 500μM H_2O_2	b
hGH + 4mM AAPH	IgG1 + 4mM AAPH	Insulin + 4mM AAPH	BSA+ 4mM AAPH	–	hGH 10μMCu(II) + 500μM L-Asc	IgG1 10μMCu(II) + 500μM L-Asc	Insulin 10μM Cu(II) + 500μM L-Asc	BSA 10μM Cu(II) + 500μM L-Asc	hGH 20μM Fe(II) + 500μM H_2O_2	IgG1 20μM Fe(II) + 500μM H_2O_2	Insulin 20μM Fe(II) + 500μM H_2O_2	b
hGH + 8mM AAPH	IgG1 + 8mM AAPH	Insulin + 8mM AAPH	BSA+ 8mM AAPH	–	hGH 20μMCu(II) + 500μM L-Asc	IgG1 20μMCu(II) + 500μM L-Asc	Insulin 20μM Cu(II) + 500μM L-Asc	BSA 20μM Cu(II) + 500μM L-Asc	–	–	–	d
hGH control	IgG1 + control	Insulin + control	BSA control	–	hGH control	IgG1 control	Insulin control	BSA control	hGH control	IgG1 control	Insulin control	e
hGH + 1mM AAPH	IgG1 + 1mM AAPH	Insulin + 1mM AAPH	BSA + 1mM AAPH	–	hGH 5μM Cu(II) + 500μM L-Asc	IgG1 5μM Cu(II) + 500μM L-Asc	Insulin 5μM Cu(II) + 500μM L-Asc	BSA 5μM Cu(II) + 500μM L-Asc	hGH 10μM Fe(II) + 500μM H_2O_2	IgG1 10μM Fe(II) + 500μM H_2O_2	Insulin 10μM Fe(II) + 500μM H_2O_2	f
hGH + 4mM AAPH	IgG1 + 4mM AAPH	Insulin + 4mM AAPH	BSA + 4mM AAPH	–	hGH 10μM Cu(II) + 500μM L-Asc	IgG1 10μM Cu(II) + 500μM L-Asc	Insulin 10μM Cu(II) + 500μM L-Asc	BSA 10μM Cu(II) + 500μM L-Asc	hGH 20μM Fe(II) + 500μM H_2O_2	IgG1 20μM Fe(II) + 500μM H_2O_2	Insulin 20μM Fe(II) + 500μM H_2O_2	g
hGH + 8mM AAPH	IgG1 + 8mM AAPH	Insulin + 8mM AAPH	BSA + 8mM AAPH	–	hGH 20μM Cu(II) + 500μM L-Asc	IgG1 20μM Cu(II) + 500μM L-Asc	Insulin 20μM Cu(II) + 500μM L-Asc	BSA 20μM Cu(II) + 500μM L-Asc	–	–	–	h
1	2	3	4	5	6	7	8	9	10	11	12	

MetSO represents one of the major degradation products in protein therapeutics, which can potentially impact protein pharmaceuticals (8,9). In addition, MetSO is frequently monitored as a representative oxidation product of protein pharmaceuticals. Typically, MetSO is detected by peptide mapping in combination with LC-MS analysis, which does not permit rapid screening of multiple formulations. Our fluorogenic assay shows that after exposure of hGH to AAPH, the amount of DOPA in oxidized hGH correlates quantitatively with the formation of MetSO which was measured by LC-MS. Based on our observations the key to this correlation is likely the parallel reaction of $ROO^{\bullet}$ with both Tyr and Met, as outlined in Scheme 3. Upon thermolysis of AAPH in air, the formation of carbon-centered radicals yields $ROO^{\bullet}$ (Scheme 2) which oxidize tyrosine to tyrosyl radicals ($TyrO^{\bullet}$, Scheme 3**, reaction 1**). $TyrO^{\bullet}$ can further react with peroxyl radicals to form DOPA (Scheme 3**, reaction 2**), which can be derivatized with ABS to form the fluorescent benzoxazole derivative (Scheme 1). In parallel, $ROO^{\bullet}$ reacts via two-electron oxidation with Met yielding MetSO and an alkoxyl radical (39) ($RO^{\bullet}$, Scheme 3**, reaction 3**). $RO^{\bullet}$ can oxidize Tyr to yield DOPA via formation of $TyrO^{\bullet}$ (Scheme 3**, reactions 4 and 5**). Because DOPA and MetSO are formed simultaneously and originate from the same oxidants (i.e. $RO^{\bullet}$, $ROO^{\bullet}$), the identification and characterization of one of these oxidation products allows for predicting the formation of the others. We note that analogous linear correlations between DOPA and MetSO formation can also be expected for other oxidants, except that the absolute values may vary depending on the preference of the specific oxidants for Tyr and Met, respectively. The only exception will be peroxides in the absence of metals, where peroxides would react nearly exclusively with Met to generate MetSO (i.e., in the absence of metals, no Fenton-type reaction is expected). However, as most proteins will show trace of metal contaminants such conditions are frequently not met in pharmaceutical formulations.

CONCLUSIONS

Our rapid fluorescence based screening allows for the fast comparison of the stability of multiple formulations, for example in 96 well plates. Subsequent in depth LC-MS analysis can then be limited to the most promising formulations, resulting in significant saving of time and resources.

Acknowledgments and Disclosures. We wish to thank Dr. Nadya Galeva of the KU Mass spectrometry/Analytical Proteomics Laboratory for performing LC-MS experiments on the LTQ-FT instrument.

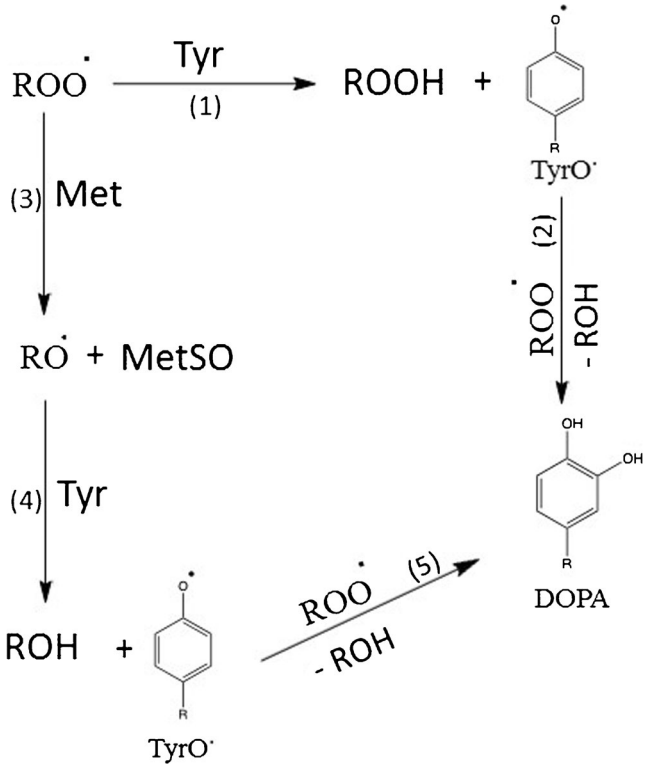

Scheme 3 Oxidation of Tyr and Met initiated by peroxyl radical

REFERENCES

1. Benjamin L, Quentin JB, Golan DE. Protein therapeutics: a summary and pharmacological classification. Nat Rev Drug Discov. 2008;7:21–39.
2. Li S, Schöneich C, Borchardt RT. Chemical instability of protein pharmaceuticals. Mechanisms of oxidation and strategies for stabilization. Biotechnol Bioeng. 1995;48:490–500.
3. Manning CM, Chou DK, Murphy MB, Payne WR, Katayama SD. Stability of protein pharmaceuticals: an update. Pharm Res. 2010;27(4):544–75.
4. Hawe A, Wiggenhorn M, Van De Weert M, Garbe HJ, Mahler HC, Jiskoot W. Forced degradation of therapeutic proteins. J Pharm Sci. 2011;101(3):895–913.
5. Wang W. Instability, stabilization, and formulation of liquid protein pharmaceuticals. Int J Pharm. 1999;185:129–88.
6. Schöneich C, Hageman JM, Borchardt TB. Stability of peptides and proteins. In K. Park (Ed.) Controlled Drug Delivery. Am Chem Soc 1997;205–28.
7. Zhong X, Neumann P, Corbo M, Loh E. Recent advances in biotherapeutics drug discovery and development. Kapetanovic M I (Ed) Drug Discovery and Development-Present and Future. INTECH 2011 (www.intechopen.com).
8. Torosantucci R, Schöneich C, Jiskoot W. Oxidation of therapeutic proteins and peptides: structural and biological consequences. Pharm Res. 2014;31:541–53.
9. Wang W, Vlasak J, Li Y, Pristatsky P, Fang Y, Pittman T, Roman J, Wang Y, Prueksaritanont T, Ionescu R. Impact of methionine oxidation in human IgG1 Fc on serum half-life of monoclonal antibodies. Mol Immunology. 2011;48:860–6.
10. Gaza-Bulesco G, Faldu S, Hurkmans K, Chumsae C, Liu H. Effect of methionine oxidation of a recombinant monoclonal antibody on the binding affinity to protein a and protein G. J Chromatogr B. 2008;870:55–62.
11. Wei Z, Feng J, Lin HY, Mullapudi S, Bishop E, et al. Identification of a single tryptophan residue as critical for binding activity in a humanized monoclonal antibody against respiratory syntical virus. Anal Chem. 2007;79:2797–805.
12. Kerwin B. Polysorbates 20 and 80 used in the formulation of protein biotherapeutics: structure and degradation pathways. J Pharm Sci. 2008;97:2924–35.
13. Donbrow M, Azaz E, Pillersdorf A. Autoxidation of polysorbates. J Pharm Sci. 1978;67:1676–81.
14. Zhou S, Mozziconacci O, Kerwin AB, Schöneich C. Fluorogenic tagging methodology applied to characterize oxidized tyrosine and phenylalanine in an immunoglobulin monoclonal antibody. Pharm Res. 2013;30:1311–27.
15. Stadtman ER, Olivier CN. Metal-catalyzed oxidation of proteins. J Biol Chem. 1991;266(4):2005–8.
16. Stadtman ER. Oxidation of free amino acid residues in proteins by radiolysis and metal- catalyzed reactions. Annu Rev Biochem. 1993;62:797–821.
17. Mozziconacci O, Ji JA, Wang J, Schöneich C. Metal-catalyzed oxidation of protein methionine residues in human parathyroid hormone (1-34): formation of homocysteine and a novel methionine-dependent hydrolysis reaction. Mol Pharm. 2012;10:739–55.
18. Chen G, Pramanik NB. Application of LC/MS to proteomics studies: current status and future prospects. Drug Discov Today. 2009;14:465–71.
19. Chen G, Warrack MB, Goodenough KA, Wei H, Wang-inverson BD, Tymiak AA. Characterization of protein therapeutics by mass spectrometry: recent developments and future developments. Drug Discov Today. 2011;16:58–64.
20. Schöneich C, Sharov VS. Mass spectrometry of protein modifications by reactive oxygen and nitrogen species. Free Radic Biol Med. 2006;41:1507–20.
21. Kaltashov IA, Bobst CE, Abzalimov RR, Wang G, Baykal B, Wang S. Advances and challenges in analytical characterization of biotechnology products: mass spectrometry-based approaches to study properties and behavior of protein therapeutics. Biotechnol Adv. 2012;30:210–22.
22. Sharov VS, Dremina ES, Galeva NA, Gerstenecker GS, Li X, Dobrowsky RT, Stobaugh JF, Schöneich C. Fluorogenic tagging of peptide and protein 3-Nitrotyrosine with 4-(amino methyl)-benzenesulfonicacid for quantitative analysis of protein tyrosine nitration. Chromatographia. 2010;71:37–53.
23. Sharov VS, Dremina ES, Pennington J, Killmer J, Asmus C, Thorson M, Hong SJ, Li X, Stobaugh JF, Schöneich C. Selective fluorogenic derivatization of 3-nitrotyrosine and 3,4-dihydroxyphenylalanine in peptides: a method designed for quantitative proteomic analysis. Methods Enzymol. 2008;441:19–32.
24. Kishore RS, Kiese S, Fischer S, Pappenberger A, Grauschopf U, Mahler H-C. The degradation of polysorbates 20 and 80 and its potential impact on the stability of biotherapeutics. Pharm Res. 2011;28(5):1194–210.
25. Betigeri S, Thakur A, Raghavan K. Use of 2-2′- Azobis (2-Amidinopropane) Dihydrochloride as a reagent tool for evaluation of oxidative stability of drugs. Pharm Res. 2005;22:310–7.
26. Werber J, Wang JY, Milligan M, Li M, Ji AJ. Analysis of 2-2′-Azobis (2- Amidinopropane) Dihydrochloride degradation and hydrolysis in aqueous solution. J Pharm Sci. 2011;100(8):3307–15.
27. Ji J, Zhang B, Cheng W, Wang JY. Methionine, tryptophan, and Histidine Oxidation in a Model protein, PTH: Mechanisms and stabilization. J Pharm Sci. 2009;98:4485–500.
28. Steinmann D, Ji JA, Wang YJ, Schöneich C. Oxidation of human growth hormone by oxygen-centered radicals: formation of Leu-101 hydroperoxides and Tyr-103 oxidation products. Mol Pharm. 2012;9:803–14.

29. Zhao F, Ghezzo-Schöneich E, Aced GI, Hong J, Milby T, Schöneich C. Metal-catalyzed oxidation of histidine in human growth hormone. Mechanism, isotope effects, and inhibition by a mild denaturing alcohol. J Biol Chem. 1997;272:9019–29.
30. Shevchenko A, Tomas H, Havli J, Olsen JV, Mann M. In-gel digestion for mass spectrometric characterization of proteins and proteomes. Nat Protoc. 2007;1:2856–60.
31. Xu H, Freitas MA. MassMatrix: a database search program for rapid characterization of proteins and peptides from tandem spectroscopy data. Proteomics. 2009;9:1548–55.
32. Mani RD, Abbatiello ES, Carr AS. Statistical characterization of multiple-reaction monitoring mass spectrometry (MRM-MS) assays for quantitative proteomics. BioMed Central. 2012;13:S9.
33. Seema B, Ajit T, Raghavan K. Use of 2,2′- Azobis(2-Amidinopropane) Dihydrochloride as a reagent tool for evaluation of oxidative stability of drugs. Pharm Res. 2005;22:310–317.
34. Hawkins CL, Davies MJ. Generation and propagation of radical reactions on proteins. Biochim Biophys Acta. 2001;1504:196–219.
35. Berges J, Trouillas P, Houee-Levin C. Oxidation of protein tyrosine or methionine residues: from the amino acid to peptide. J Phys Conf Ser. 2011;261
36. White RE. High-throughput screening in drug metabolism and pharmacokinetic support of drug discovery. Annu Rev Pharmacol Toxicol. 2000;40:133–57.
37. Capelle M, Gurny R, Arvinte T. High throughput screening of protein formulation stability: practical considerations. Eur J Pharm Biopharm. 2007;65:131–48.
38. Niki E. Free radical initiators as source of water-or lipid-soluble peroxyl radicals. Methods Enzymol. 1990;186:100–8.
39. Schöneich C. Methionine oxidation by reactive oxygen species: reaction mechanisms and relevance to Alzheimer's disease. Biochim Biophys Acta. 2005;1703(2):111–9.